

Using paired visual and passive acoustic surveys to estimate passive acoustic detection parameters for harbor porpoise abundance estimates

Eiren K. JacobsonKarin A. ForneyJay Barlow

Citation: *J. Acoust. Soc. Am.* **141**, 219 (2017); doi: 10.1121/1.4973415

View online: <http://dx.doi.org/10.1121/1.4973415>

View Table of Contents: <http://asa.scitation.org/toc/jas/141/1>

Published by the [Acoustical Society of America](#)

Using paired visual and passive acoustic surveys to estimate passive acoustic detection parameters for harbor porpoise abundance estimates

Eiren K. Jacobson^{a)}

Scripps Institution of Oceanography, 9500 Gilman Drive, La Jolla, California 92093-0208, USA

Karin A. Forney

National Oceanographic and Atmospheric Administration, National Marine Fisheries Service, Southwest Fisheries Science Center, 110 Shaffer Road, Santa Cruz, California 95060, USA

Jay Barlow

National Oceanographic and Atmospheric Administration, National Marine Fisheries Service, Southwest Fisheries Science Center, 8901 La Jolla Shores Drive, La Jolla, California 92037, USA

(Received 29 April 2016; revised 7 December 2016; accepted 8 December 2016; published online 13 January 2017)

Passive acoustic monitoring is a promising approach for monitoring long-term trends in harbor porpoise (*Phocoena phocoena*) abundance. Before passive acoustic monitoring can be implemented to estimate harbor porpoise abundance, information about the detectability of harbor porpoise is needed to convert recorded numbers of echolocation clicks to harbor porpoise densities. In the present study, paired data from a grid of nine passive acoustic click detectors (C-PODs, Chelonia Ltd., United Kingdom) and three days of simultaneous aerial line-transect visual surveys were collected over a 370 km² study area. The focus of the study was estimating the effective detection area of the passive acoustic sensors, which was defined as the product of the sound production rate of individual animals and the area within which those sounds are detected by the passive acoustic sensors. Visually estimated porpoise densities were used as informative priors in a Bayesian model to solve for the effective detection area for individual harbor porpoises. This model-based approach resulted in a posterior distribution of the effective detection area of individual harbor porpoises consistent with previously published values. This technique is a viable alternative for estimating the effective detection area of passive acoustic sensors when other experimental approaches are not feasible.

[<http://dx.doi.org/10.1121/1.4973415>]

[JFL]

Pages: 219–230

I. INTRODUCTION

Fixed passive acoustic technologies are promising tools for long-term assessment of cetacean populations (Mellinger *et al.*, 2007). However, to use passive acoustic sensors to estimate cetacean density and abundance, the probability of detecting individuals must be known or estimated (Marques *et al.*, 2009). There are two components of this detectability: (1) the rate at which animals produce sounds and (2) the probability of detecting sounds produced at varying distances from the passive acoustic sensor (the detection function). In wild animal populations, the sound production rates of individuals and the detection functions of passive acoustic sensors are difficult to measure experimentally. Rather than directly measuring these quantities, we used simultaneous visual surveys and a deployment of passive acoustic sensors to create a paired dataset that allowed us to estimate the product of the sound production rate and the area monitored by the passive acoustic sensors, which we refer to as the effective detection area (EDA). This paper uses a harbor porpoise population in California as a case study to present a new approach for determining a conversion factor between sounds detected

and animal density that can be used for long-term passive acoustic monitoring (PAM) of animal abundance.

Along the central and northern California coast, harbor porpoise (*Phocoena phocoena*) occur in four distinct populations (Calambokidis and Barlow, 1991; Chivers *et al.*, 2002). Harbor porpoises in this region are distributed in areas with bottom depths less than 100 m, with greatest densities where bottom depths are 10–40 m (Barlow, 1988; Carretta *et al.*, 2001; Forney *et al.*, 2001). Due to their nearshore distribution, harbor porpoise are exposed to a diverse array of lethal and sublethal anthropogenic impacts including pollution, noise, and fishery interactions (Barlow and Forney, 1994). In some areas, cumulative anthropogenic impacts have led to the decline or disappearance of harbor porpoise populations (Calambokidis *et al.*, 1984). For example, harbor porpoises disappeared from the San Francisco Bay and the Puget Sound in the mid-20th century, possibly due to high concentrations of toxic chemicals (Calambokidis *et al.*, 1985; Raum-Suryan and Harvey, 1998) and have only recently repopulated these areas (Keener *et al.*, 2011; Anderson, 2014).

In central California, harbor porpoises were caught incidentally in set gillnets targeting halibut from the 1960s to the 1990s, with particularly high take in the 1980s (Barlow and Forney, 1994; Jefferson *et al.*, 1994). Due to this

^{a)}Electronic mail: eiren.jacobson@gmail.com

incidental take, the central California population may have been reduced by as much as 70% of their pre-bycatch abundance (Barlow and Hanan, 1995). Currently, all California populations are believed to be either stable or recovering from past gillnet take (Forney *et al.*, 2014). The abundance of the Monterey Bay harbor porpoise population was most recently estimated to be 3715 [Coefficient of Variation (CV) = 0.51; Forney *et al.*, 2014]. Fishery mortality is currently considered to be insignificant for this stock, and there are no known habitat issues (Carretta *et al.*, 2015); however, over the past decade there has been some mortality due to bottlenose dolphin (*Tursiops truncatus*) attacks on harbor porpoise in this region (Cotter *et al.*, 2011; Wilkin *et al.*, 2012; Jacobson *et al.*, 2014).

Harbor porpoise populations in California have been monitored using aerial surveys since the late 1980s; however, these surveys are expensive, restricted by weather, and have a limited ability to detect trends in harbor porpoise abundance (Forney *et al.*, 1991). Fixed PAM, which has been used successfully elsewhere (e.g., Gallus *et al.*, 2012) might be more effective for monitoring harbor porpoise populations in this region.

Harbor porpoise produce highly directional echolocation clicks with peak frequencies around 130 kHz (Au *et al.*, 1999) that are used for navigation, foraging, and communication (Akamatsu *et al.*, 2007; Clausen *et al.*, 2010; Linnenschmidt *et al.*, 2012; Wisniewska *et al.*, 2016). These clicks attenuate rapidly in seawater, resulting in an active acoustic space of several hundred meters (DeRuiter *et al.*, 2010). Because harbor porpoise echolocation clicks are well described and do not travel long distances, they can be used as a proxy for animal density around a passive acoustic sensor.

One passive acoustic sensor that has been widely used to study harbor porpoise is the C-POD (Tregenza (2012), Chelonia Ltd., United Kingdom, www.chelonia.co.uk). C-PODs are relatively inexpensive, easy to operate, and can be deployed for 3–6 months at a time. C-PODs detect individual echolocation clicks and store digital summary information about each click. No waveform data are collected. In post-processing, clicks can be classified as likely to have been produced by a harbor porpoise using characteristics including the peak frequency and duration of clicks along with the inter-click interval.

Metrics of harbor porpoise occurrence derived from passive acoustic data have been shown to correlate positively with density estimates derived from visual observations (e.g., Kyhn *et al.*, 2012; Williamson *et al.*, 2016). C-PODs and their predecessors, the POD and T-POD, have been used to document harbor porpoise habitat use (e.g., Carlstrom, 2005; Verfuß *et al.*, 2007), to monitor the impacts of anthropogenic activities (e.g., Carstensen *et al.*, 2006; Brandt *et al.*, 2011; Dähne *et al.*, 2013a; Thompson *et al.*, 2013; Brandt *et al.*, 2014) and to assess population abundance and trend (Gallus *et al.*, 2012; Jaramillo-Legorreta *et al.*, 2016).

To convert echolocation clicks detected by C-PODs to animal densities, a detection function is needed to describe the probability of detection as a function of distance from the C-POD (Buckland *et al.*, 2001; Marques *et al.*, 2013).

Traditionally, it is assumed that animals at zero distance from the sensor are detected with certainty (Buckland *et al.*, 2001); however, because harbor porpoises produce highly directional echolocation clicks, and because they do not click continuously, the probability of detection at zero distance is less than one. Therefore, the click rate of individual porpoises is needed to scale the detection function appropriately. From these two pieces of information we can estimate the EDA of the C-POD.

Kyhn *et al.* (2012) used paired visual and PAM sessions in a mark-recapture framework to estimate the detection functions of individual T-PODs in an area with relatively low harbor porpoise densities where individual porpoises could be visually tracked. Using these paired data, they estimated the effective detection radii of individual T-PODs to be between 22 and 104 m. C-PODs have been found to be less variable in sensitivity than T-PODs (Dähne *et al.*, 2013b) and thus we would expect the range of detection radii for individual C-PODs to be narrower, though this has not yet been shown experimentally. One recent experiment tracked harbor porpoises in three dimensions as they moved through a closely spaced array of sensors; however, this approach to estimating the detection function was foiled in part by the extremely high directionality of harbor porpoise echolocation, resulting in very few simultaneous detections on multiple sensors required for estimation of a detection function using this approach (Koblitz, 2015).

To estimate the echolocation click rate of individual porpoises, researchers in Denmark affixed acoustic sensors to wild harbor porpoises and found that harbor porpoise echolocate almost continuously (Akamatsu *et al.*, 2007; Linnenschmidt *et al.*, 2012; Wisniewska *et al.*, 2016). However, individual variation in reported echolocation activity was sometimes large, and the small sample size inherent to tagging studies (<10 animals in total) makes it difficult to extrapolate results to an entire population or species.

In the present study, we did not attempt to estimate the detection function and the echolocation click rate independently; instead, we treated the EDA as an unknown quantity that allows conversion from passive acoustic data to animal density. By using an established visual method to estimate harbor porpoise density in our study area at the same time that passive acoustic sensors were deployed, we were able to solve for the unknown EDA. This allowed us to estimate harbor porpoise density in our study area using passive acoustic data at times when visual surveys were not conducted.

II. MATERIALS AND METHODS

This section describes how passive acoustic and visual survey data were collected, provides an overview of data processing and analytical techniques, and explains how the two datasets were combined in a Bayesian model framework to estimate the EDA of the passive acoustic instruments. Finally, we show how the estimated EDA can be applied to long-term passive acoustic datasets to estimate harbor porpoise abundance.

A. Data collection

1. Passive acoustic methods

In 2013, we installed a grid of PAM devices (C-PODs) in northern Monterey Bay (Fig. 1). We deployed 11 C-PODs at the end of August 2013 and retrieved 10 C-PODs during the first week of January 2014. For this experiment, we chose Monterey Bay as our study site because the local population of harbor porpoises is relatively well studied and believed to be stable (Carretta *et al.*, 2015). The bathymetry of northern Monterey Bay results in a rapid spatial gradient of harbor porpoise densities, with relatively high densities in the nearshore areas and relatively low densities near the deep Monterey Canyon. The study area included waters from 10 to 100m depth, north of 36.8° N and east of 122.10° W, with a total area of 370 km^2 . Our study area represents approximately 15% of the Monterey Bay harbor porpoise stock range (Forney *et al.*, 2014), but has a disproportionately high density of harbor porpoises relative to the rest of the region occupied by this population. The study design was a systematic, randomly positioned offset grid of 11 C-PODs spaced 0.035° latitude and 0.07° longitude apart and oriented to follow the shape of the coastline. As a result of this design, the lateral distance between instruments was 3.4 km, the medial distance was 2.1 km, and the diagonal distance was 2.7 km.

2. Aerial survey methods

Three replicate fine-scale aerial surveys were flown over the northern Monterey Bay study area during the C-POD grid deployment on October 15, 17, and 31, 2013 (Fig. 1). The exact dates of the aerial surveys were determined by suitable weather conditions. These simultaneous surveys were designed to estimate the density and abundance of harbor porpoise in the 370 km^2 study area. Aerial surveys covered a randomly placed, systematic set of 20 east–west transect lines spaced 0.0083° (960 m) apart that were designed independently from the grid of C-POD moorings. The coverage of the line transects was restricted in part by logistical constraints; this level of coverage was realizable in a single attempt given limited calm weather windows and an approximate 4-h flight time due to fuel capacity. Surveys were conducted from a Partenavia P-68 high-wing twin-engine aircraft using standard aerial line-transect survey methods (Forney *et al.*, 1991). In summary, two observers searched from bubble windows on either side of the aircraft while a third observer searched from a belly window in the rear of the aircraft. A data recorder transcribed verbal sighting information for cetaceans and turtles (including declination angle, species, and number of animals) and environmental (visibility conditions) information from the observers into a custom-written software program on a laptop computer (Toshiba T-1000, Japan) that was directly connected to a hand-held Global Positioning System (Garmin 12XL, USA).

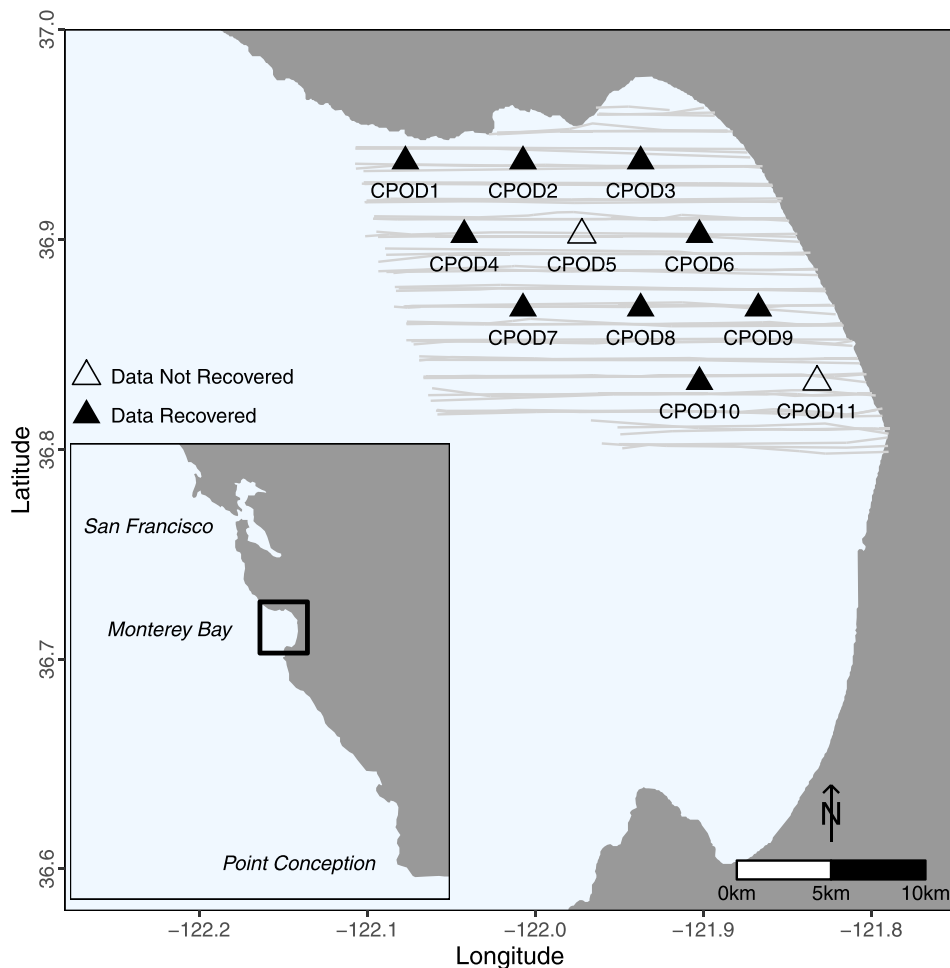


FIG. 1. (Color online) Completed replicates of aerial survey line transects (gray lines) and C-POD deployment locations (triangles) in Monterey Bay, California. C-PODs from which data were successfully recovered in 2013 are indicated by filled triangles, while open triangles indicate C-PODs that did not return data.

B. Analytical methods

1. C-POD data processing

Once the C-PODs were recovered, data were processed using the KERNO algorithm in the program CPOD.exe (v. 2.044; Tregenza, 2012) to detect click trains. All narrow-band, high-frequency (NBHF) click trains were classified as belonging to harbor porpoise, and we chose to include only high-quality click trains (as defined by the KERNO algorithm) in our analysis in order to minimize false positives in the dataset. High-quality NBHF click trains detected on the three days of acoustic effort considered in the present study were visually validated. No false positives were detected in the dataset. While Dall's porpoise (*Phocoenoides dalli*) also occur along the U.S. West Coast and produce very similar NBHF echolocation signals, we are confident that our dataset includes only harbor porpoise echolocation click trains because Dall's porpoise are typically found in water hundreds to thousands of m deep (Forney, 2000) and because no Dall's porpoise were sighted in our study area during the aerial surveys conducted as part of this study or in any other aerial surveys conducted in 2011 or 2013. Data were exported from CPOD.exe and all further analyses were performed in R (v. 3.2.2; R Core Team, 2016).

We considered a variety of passive acoustic metrics, including counts of echolocation clicks (e.g., Bailey *et al.*, 2010; Marques *et al.*, 2009) and of echolocation click-positive intervals (e.g., Brandt *et al.*, 2011; Williamson *et al.*, 2016), over periods of seconds, minutes, hours, and days. We found that counts of individual echolocation clicks tended to be overdispersed, and because the click production rates of individual porpoises are so variable (Akamatsu *et al.*, 2007; Linnenschmidt *et al.*, 2012; Wisniewska *et al.*, 2016) we did not feel confident that the number of echolocation clicks per time would scale linearly with the number of animals present. Because our goal was to estimate the number of individuals, not groups, we could not use metrics like detection positive minutes or hours where more than one individual would likely be detected, which would result in biased estimates of density and abundance. We chose to use the proportion of porpoise positive seconds (PPS) as our passive acoustic metric because this metric is less likely to become saturated when multiple animals are present and because it reduces the impact of animal orientation on detectability by effectively averaging over 1-s periods. Our methods assume that only one porpoise can be detected within any 1-s period, which is likely given the narrow beam width of harbor porpoises and the resulting rapid changes in detectability with animal movement and orientation (Koblitz *et al.*, 2012). To determine the time period over which PPS should be calculated, we calculated PPS for 3-, 6-, and 12-h intervals and correlated these values with the corresponding density estimates from the aerial surveys (see Sec. IIB 3 for details). While PPS calculated over a 3-h period had the highest correlation with the aerial survey dataset, a large proportion of the acoustic data points (17/27) were zeros. The second highest correlation was with 12-h periods and produced fewer (6/27) zeros in the acoustic dataset. This metric

also makes biological sense since diel changes in echolocation behavior have been reported for this species (Carlstrom, 2005). Therefore, we calculated the PPS recorded by each C-POD during daylight hours (between civil dawn and dusk, approximately 7 a.m. to 7 p.m. PST) on each of the days on which aerial surveys were flown.

2. Estimating harbor porpoise densities using distance sampling

Aerial survey line transect effort was divided first into segments with continuous effort in constant sighting conditions (Beaufort sea state) and then divided again into 1-km effort subsegments. Following Becker *et al.* (2010), when it was not possible to divide effort segments exactly into 1-km subsegments, if the remainder of the effort segment was less than 500 m it was added randomly to one of the subsegments, while if the remainder was greater than 500 m a new subsegment was created and positioned randomly into the effort segment. Due to the low probability of observing harbor porpoise in high sea states, only data from the aerial survey effort obtained in Beaufort sea states 0–3 were included. We used the package Distance (v. 0.9.4; Miller, 2015) to fit a detection function to the aerial survey data using a half-normal key function with cosine adjustments. We considered models with and without Beaufort sea state as a covariate and used Akaike's Information Criterion (AIC) to select the best model.

For each subsegment of aerial survey effort, the point density of the harbor porpoise at the midpoint of that subsegment was calculated as

$$d = \frac{\text{no. harbor porpoise}}{\text{segment length} \times \text{ESW}_{\text{BF}}}, \quad (1)$$

where ESW_{BF} is the Beaufort-specific effective strip width. This calculation does not include a correction for the probability of seeing animals directly on the trackline, $g(0)$. In traditional line-transect methods, it is assumed that $g(0) = 1$; however, since cetaceans spend time below the sea surface where they are not detectable by visual observers, $g(0)$ for cetaceans can be considerably less than 1 (Buckland *et al.*, 2001). Our dataset did not allow us to estimate $g(0)$, but a previous study by Laake *et al.* (1997) derived an estimate of $g(0)$ for harbor porpoise in a different region from the same aircraft using the same survey methods under similar survey conditions. Rather than applying this estimate of $g(0)$ directly, we chose to include it as a parameter to be estimated in our Bayesian model in Sec. IIB 3 based on prior information (point estimate and associated uncertainty) from Laake *et al.* (1997).

3. Estimating harbor porpoise densities at C-POD locations

To estimate the density of harbor porpoises at the locations of C-POD moorings on each day of aerial surveys, we needed to interpolate the aerial survey observations across the study area. Previously, splines have been used to interpolate discrete observations smoothly to estimate average

spatial density (e.g., Forney *et al.*, 2012). Splines create the smoothest possible interpolation and can be useful for visualizing average cetacean densities over long time scales (e.g., seasons, decades; see Becker *et al.*, 2012). In our application, we wished to estimate the spatial density of harbor porpoises separately for each day of aerial survey effort. Splines do not consider the data covariance, which is low over short time scales due to patchy harbor porpoise distributions. To preserve the observed patchiness in the spatial distribution of harbor porpoises, we used a least-squares approach known as objective mapping or Gauss-Markov smoothing (Gandin, 1965; Bretherton *et al.*, 1976; Thomson and Emery, 2014) to estimate the spatial density of harbor porpoises across the study area on each day of aerial survey effort. This technique uses the covariance of the harbor porpoise density data over space to determine the length scales of interpolation and seeks to minimize the interpolation error variance (McIntosh, 1990). Using this objective interpolation technique, we estimated the density of harbor porpoises with associated error at the location of each C-POD on each of the days on which aerial surveys were conducted. It would be preferable to estimate the density of a harbor porpoise within the EDA of each C-POD; however, the EDA of the C-PODs is not known.

4. Bayesian estimation of unknown acoustic detection parameters

Following Marques *et al.* (2009), the proportions of PPS recorded are related to the aerial survey density estimates at each C-POD on each day by the equation

$$\frac{\hat{D}_{m,d}}{\hat{g}(0)} = \frac{n_{m,d}}{T_{m,d}\hat{v}\hat{p}}, \quad (2)$$

where $\hat{D}_{m,d}$ is the estimated harbor porpoise density (km^{-2}) from the objective interpolation of aerial survey density estimates as estimated for each C-POD location m on each day d . $\hat{g}(0)$ is an informed prior (taken from Laake *et al.*, 1997) on the probability of detecting animals directly on the trackline. $n_{m,d}$ are the number of PPS recorded by each mooring m on each day d , and $T_{m,d}$ is the time (in seconds) monitored between dawn and dusk. $\hat{v}\hat{p}$ is an uninformed prior on the product of \hat{v} , the EDA of the C-POD, and \hat{p} , the probability of echolocating within a 1-s period for individual harbor porpoises.

For modeling purposes, we rearranged the equation to solve for $n_{m,d}$,

$$n_{m,d} = \frac{\hat{D}_{m,d}}{\hat{g}(0)} \times T_{m,d} \times \hat{v}\hat{p}. \quad (3)$$

The passive acoustic data, $n_{m,d}$, were modeled using an overdispersed negative binomial distribution. The parameters of interest to us are \hat{v} and \hat{p} . Based on previous research (DeRuiter *et al.*, 2010), we consider \hat{v} to fall between 0 and 0.0314 km^2 (corresponding to radii of 0 to 100 m). Since \hat{p} is a probability, it must fall between 0 and 1.

Due to the high level of uncertainty in the density estimates $\hat{D}_{m,d}$ calculated from the objective analysis of aerial survey data, these estimates were included with their errors and were also estimated by the Bayesian model. $\hat{D}_{m,d}$ were highly informed priors; each $\hat{D}_{m,d}$ was drawn from a lognormal distribution according to the density estimate and associated uncertainty for each C-POD location on each day.

The probability of seeing a harbor porpoise directly on the trackline, $\hat{g}(0)$, has been estimated by Laake *et al.* (1997). In our model $\hat{g}(0)$ was added as a multiplier with a prior distribution based on the estimate from Laake *et al.* [$\mu = 0.292$, standard error (SE) = 0.107] converted to a beta distribution.

We implemented this model using the package R2jags (v. 0.5–7; Su and Yajima, 2015). Our model run included 250 000 Markov Chain Monte Carlo samples on four parallel chains, with a burn-in period of 50 000 samples and tenfold thinning.

5. Density estimation using passive acoustic data

To evaluate whether our estimate of $\hat{v}\hat{p}$ was consistent with previous studies, we explored the parameter space of \hat{v} and \hat{p} consistent with the model estimate. Further, we constructed daily and monthly passive acoustic estimates of harbor porpoise abundance in our study area according to Eq. (2) and compared them to the visual estimates of abundance from our aerial survey dataset. Analytical lognormal 95% confidence intervals were calculated for both the passive acoustic and visual estimates of abundance using the delta method (Seber, 1982; Marques *et al.*, 2009) to incorporate error in the estimates of $\hat{g}(0)$ and $\hat{v}\hat{p}$. To illustrate how PAM could be used to monitor trends in abundance when knowledge of absolute abundance is not required, we also calculated passive acoustic estimates of abundance assuming that $\hat{g}(0)$ and $\hat{v}\hat{p}$ were fixed at their median values, so that only variability in the passive acoustic data contributed to the uncertainty of the abundance estimates.

III. RESULTS

A. Data collection

1. Passive acoustic data collected

We deployed a grid of 11 C-PODs in north Monterey Bay at the end of August 2013 and retrieved 10 C-PODs during the first week of January 2014. One mooring became accidentally entangled in fishing gear and was retrieved and returned to us in mid-December 2013. Of our 11 C-PODs, nine instruments returned data (Fig. 1). During daylight hours on the dates when aerial surveys were flown, the nine C-PODs detected a total of 640 high-quality echolocation click trains for a total of 15 717 echolocation clicks. Individual instruments detected between 0 and 97 click trains per day, or between 0 and 2341 echolocation clicks. The resulting number of PPS during daylight hours ranged from 0 to 114 s (Table I), with proportions of PPS per time between 0 and 0.0027 (Fig. 2). In general, instruments

TABLE I. Predicted porpoise densities [PPSQKM (km^{-2}) with associated CVs] at each C-POD location (reported in X and Y m from the centroid of the study area) and observed porpoise positive seconds (PPS) on each year-day (YDay) of monitoring (T = seconds monitored) corresponding to an aerial overflight.

Mooring	X	Y	YDay	PPSQKM	CV	PPS	T
CPOD1	-11499	6273	288	0.05	50.02	0	43 680
CPOD1	-11499	6273	290	0.43	9.19	0	43 380
CPOD1	-11499	6273	304	0.1	34.17	0	41 640
CPOD2	-5278	6273	288	0.16	13.77	3	43 680
CPOD2	-5278	6273	290	3.36	1.16	5	43 380
CPOD2	-5278	6273	304	0.88	3.78	112	41 640
CPOD3	944	6273	288	2.05	1.1	5	43 680
CPOD3	944	6273	290	0.6	6.49	27	43 380
CPOD3	944	6273	304	0.33	10.08	58	41 640
CPOD4	-8392	2381	288	0.04	61.77	29	43 680
CPOD4	-8392	2381	290	0.09	40.88	4	43 380
CPOD4	-8392	2381	304	0.62	5.37	0	41 640
CPOD5	-2168	2381	288	0.52	4.35	NA	0
CPOD5	-2168	2381	290	0.18	21.4	NA	0
CPOD5	-2168	2381	304	0.06	50.76	NA	0
CPOD6	4056	2381	288	4.24	0.53	114	43 680
CPOD6	4056	2381	290	8.74	0.45	99	43 380
CPOD6	4056	2381	304	5.99	0.55	53	41 640
CPOD7	-5283	-1511	88	0.4	5.61	9	43 680
CPOD7	-5283	-1511	290	0.77	4.93	18	43 380
CPOD7	-5283	-1511	304	0.42	7.97	0	41 640
CPOD8	945	-1511	288	1.43	1.59	66	43 680
CPOD8	945	-1511	290	1.64	2.37	32	43 380
CPOD8	945	-1511	304	0.24	13.93	33	41 640
CPOD9	7172	-1511	288	0.91	2.51	28	43 680
CPOD9	7172	-1511	290	15.25	0.25	55	43 380
CPOD9	7172	-1511	304	0.83	4.03	19	41 640
CPOD10	4060	-5403	288	0.02	119	9	43 680
CPOD10	4060	-5403	290	0.09	42.24	1	43 380
CPOD10	4060	-5403	304	0.09	39.28	0	41 640
CPOD11	10290	-5403	288	0.03	88.95	NA	0
CPOD11	10290	-5403	290	0.2	18.56	NA	0
CPOD11	10290	-5403	304	1.34	2.51	NA	0

moored in shallow water recorded higher levels of echolocation activity than those moored in deeper water.

2. Aerial survey data collected

We flew the planned aerial survey tracklines once each on October 15, 17, and 31, 2013, resulting in three replicate aerial surveys in our 370 km^2 study area (Fig. 3). During these three days of aerial surveys, we completed 1228 km of effort in good conditions and observed a total of 245 groups of harbor porpoises. Seventy-two groups were observed on October 15, 104 groups were observed on October 17, and 69 groups were observed on October 31. The mean size of harbor porpoise groups was two individuals. On each of the three survey days, 35%–38% of the study area was effectively searched, based on the estimated ESW of the aerial survey (see below).

B. Analytical results

1. Estimates of harbor porpoise density

We combined the data from our three replicate aerial surveys to estimate the abundance of harbor porpoises in our

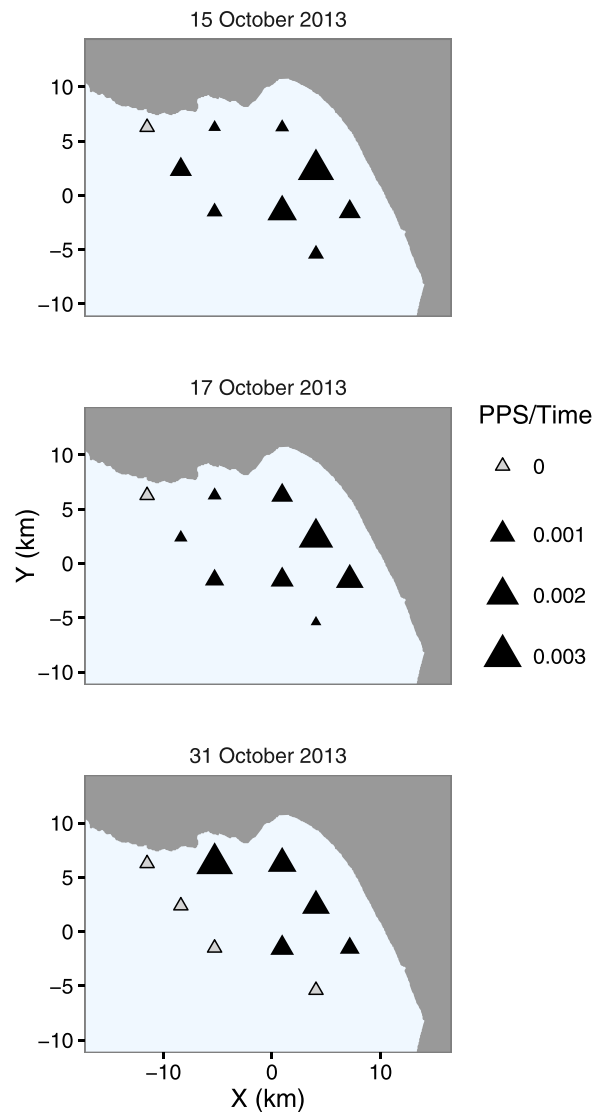


FIG. 2. (Color online) Proportion of seconds between dawn and dusk (approximately 7 a.m. to 7 p.m. PST) during which harbor porpoise were detected acoustically (PPS) by each of nine C-PODs (triangles) on each of the three days when aerial surveys were flown over the study area. Gray triangles indicate instruments that did not detect any high-quality harbor porpoise echolocation clicks, while black triangles are scaled with the non-zero PPS calculated from the C-POD data.

study area. Our estimate, corrected for $g(0)$ using the estimate from Laake *et al.* (1997) for purposes of comparison, was $N = 1446$ ($CV = 0.18$) resulting in an average density of 3.9 km^{-2} within the northern Monterey Bay study area. This harbor porpoise abundance estimate is consistent with an independent estimate using the same aerial survey methods of $N = 3715$ harbor porpoises in the entire Monterey Bay population (Forney *et al.*, 2014). Using AIC, we determined that fitting separate detection functions for Beaufort sea states 0–1 and 2–3 ($AIC = 2707$) was preferable to both a model that ignored Beaufort sea state ($AIC = 2711$) and a model which fit separate detection functions for each Beaufort sea state ($AIC = 2709$). The effective strip half-width values for our aerial surveys were 180 m for Beaufort sea states 0–1 and 134 m for Beaufort sea states 2–3. Point densities calculated at individual subsegments ranged from 0 to 42 km^{-2} prior to correction for $\hat{g}(0)$ (see Fig. 3).

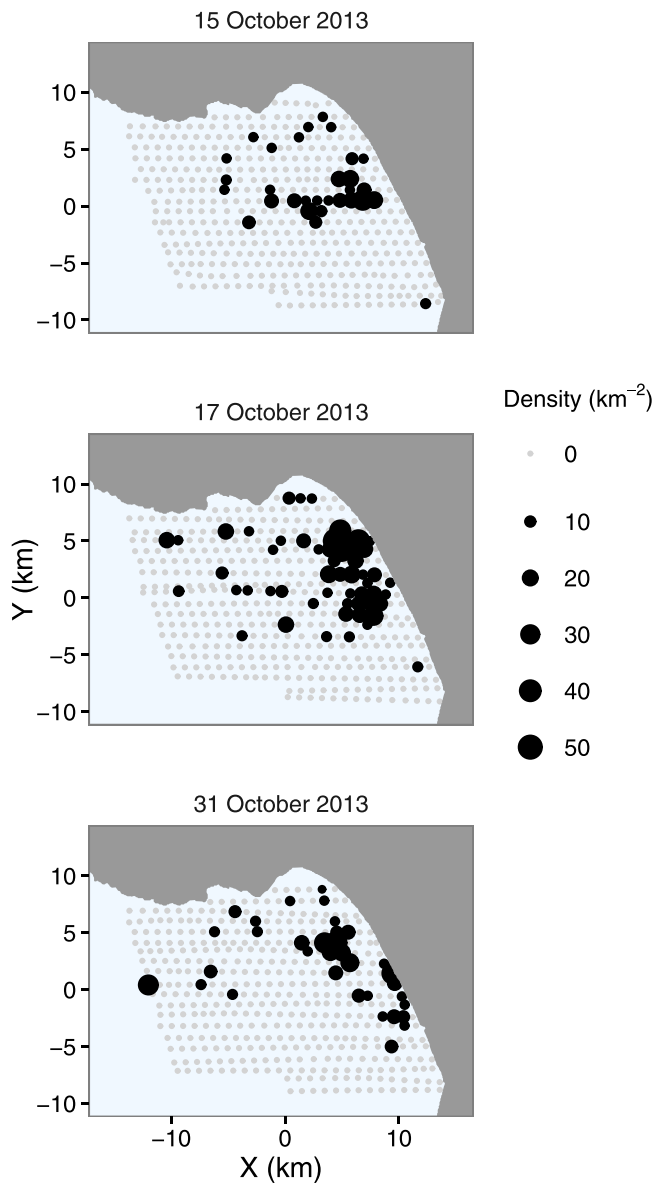


FIG. 3. (Color online) Calculated harbor porpoise point density [uncorrected for $\hat{g}(0)$] at the midpoint of each 1 km aerial survey effort subsegment. Gray circles indicate effort segments where the calculated density was zero, while black circles are scaled with non-zero densities.

2. Maps of interpolated harbor porpoise density

We used objective interpolation to estimate the spatial density of a harbor porpoise across our study area. This allowed us to estimate the density of a harbor porpoise at the point locations of each of the C-PODs on each day that aerial surveys were flown.

The interpolated values of harbor porpoise density ranged from 0 to 66 km^{-2} (Fig. 4). The interpolated densities at individual C-POD locations ranged from 0.06 to 16 km^{-2} (Table I). As is typical with aerial survey data, we observed high levels of uncertainty associated with our density estimates (Table I). The distance between each C-POD and the closest aerial survey effort subsegment ranged from 100 to 500 m. The first zero crossing of the autocorrelation of harbor porpoise density observed on aerial survey effort subsegments was between 6 and 8 km. Since the distance between

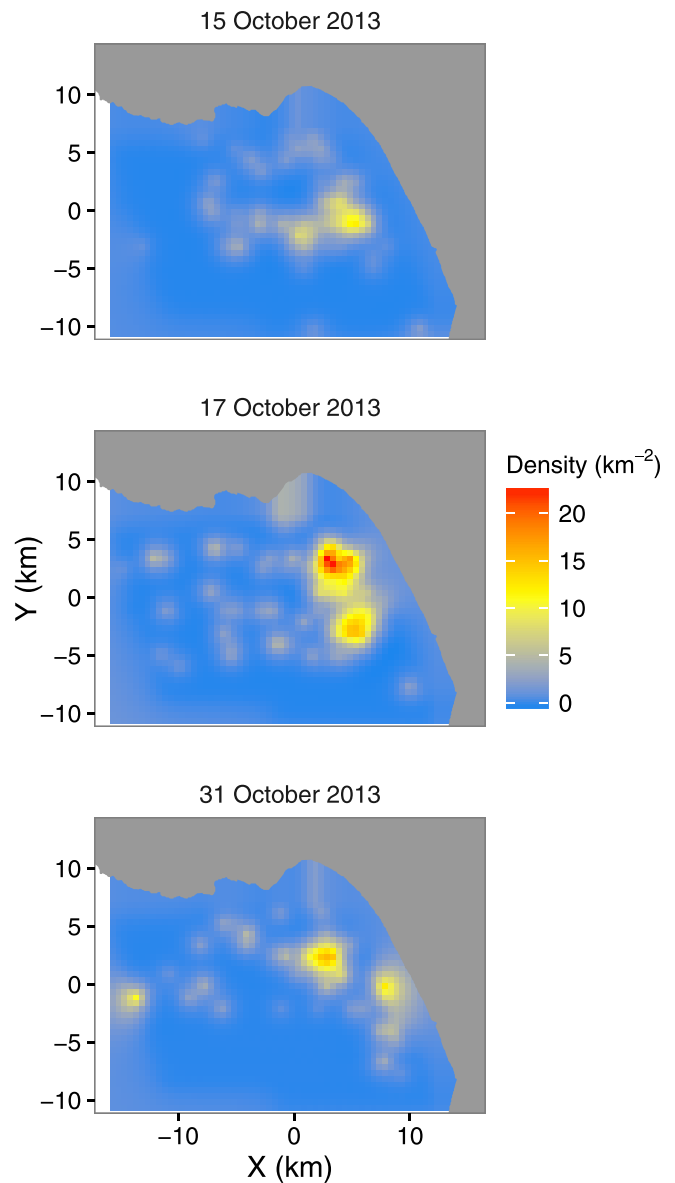


FIG. 4. (Color online) Objective interpolation of harbor porpoise density (km^{-2}) constructed using aerial survey density estimates from three days of aerial surveys in northern Monterey Bay. Note that the reported densities are uncorrected for $\hat{g}(0)$.

C-PODs and the nearest aerial survey subsegment fell well within the autocorrelation range of the aerial survey data, we felt confident using objective interpolation to interpolate aerial survey data across our study area. Harbor porpoise density estimates at individual C-PODs were positively correlated with PPS recorded during daylight hours on the days on which aerial surveys were flown ($R^2 = 0.46$; Fig. 5).

3. Bayesian estimation of unknown acoustic detection parameters

We constructed a Bayesian model to combine our visual and acoustic data with previously published information. This was an effective way to incorporate documented uncertainty in our dataset and in previous studies into our analysis.

The posterior distribution of $\hat{g}(0)$ estimated by our model was very similar to the prior distribution and had a

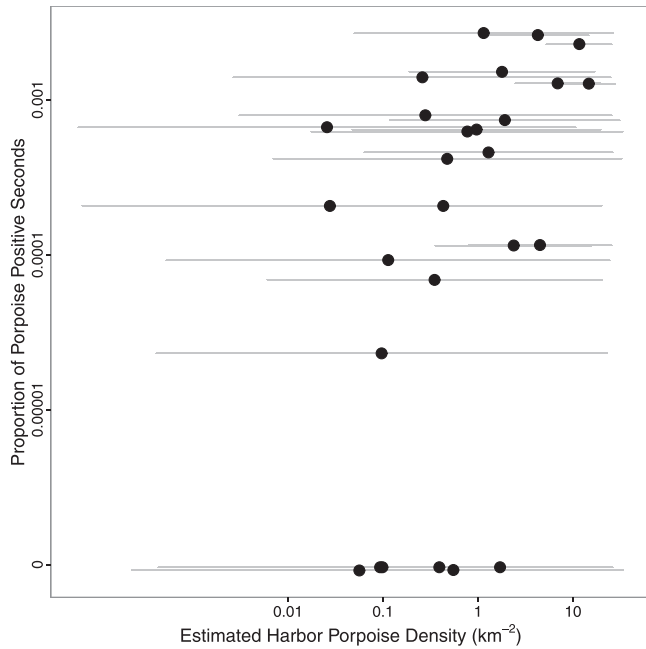


FIG. 5. Harbor porpoise densities at each C-POD location on each day ($N = 27$) as estimated by objective interpolation of aerial survey density estimates with associated 95% confidence intervals (x axis) and the proportion of PPS recorded by each C-POD between dawn and dusk on the three days of the simultaneous aerial surveys (y axis). Note that the reported porpoise densities are uncorrected for $\hat{g}(0)$.

mean of 0.33, a median of 0.32, and a standard deviation of 0.11 (Fig. 6). Since we did not provide any new information regarding $\hat{g}(0)$ to the model, this result is not unexpected. The posterior distribution of the EDA, $\hat{v}p$, had a mean of 0.001 km^2 , a median of $7 \times 10^{-4} \text{ km}^2$, and a standard

deviation of 0.001 km^2 . This result was very different from the mean and standard deviation of the prior distribution given to the model (Fig. 6).

Since we estimated the product of the detection area (\hat{v}) and the probability of clicking within a 1-s period (\hat{p}), we are unable to resolve the true values of either parameter. However, we plotted the parameter space consistent with our estimate of $\hat{v}p$ in terms of \hat{v} and \hat{p} (Fig. 7). If the true value of \hat{v} were very small, we would expect \hat{p} to be large. Conversely, if the true value of \hat{v} were very large, we would expect the true value of \hat{p} to be small. For example, if we knew the true detection radius \hat{v} to be 50 m, we could estimate the probability of clicking within each 1-s period \hat{p} to be, on average, 0.08.

The prior and posterior distributions of individual density estimates associated with each C-POD on each day of aerial surveys are shown in Fig. 8. Estimates that did not overlap the one-to-one line indicate that the posterior density estimate was considerably different from the estimate provided as a prior.

IV. DISCUSSION

Our objective was to use paired visual and passive acoustic surveys to estimate the EDA of C-PODs for the harbor porpoise in Monterey Bay, CA. Using a Bayesian modeling framework, we combined visual and passive acoustic survey data with previously published information to estimate the unknown EDA. With this estimate of the EDA, we were able to estimate harbor porpoise abundance in our study area using passive acoustic data collected over a 3-month period. The approach outlined here can be applied

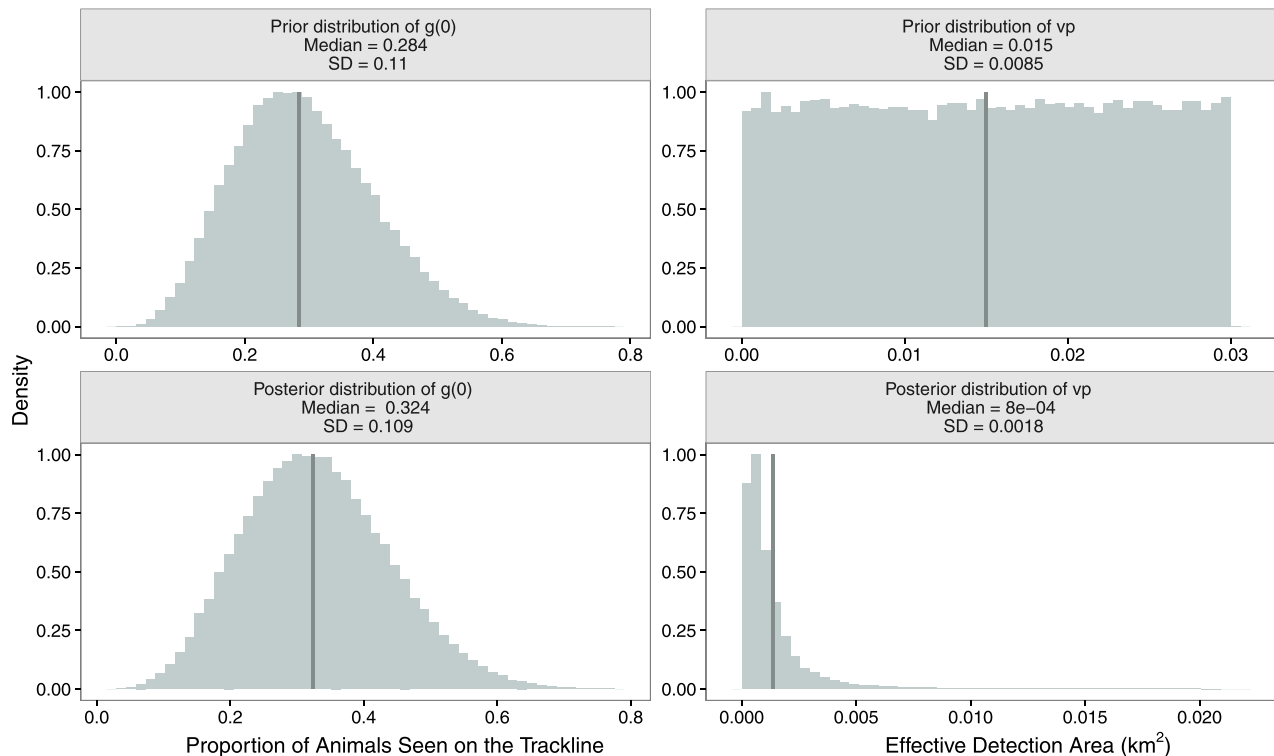


FIG. 6. (Color online) Prior (upper panels) and posterior (lower panels) distributions of $\hat{g}(0)$ (upper panels) and $\hat{v}p$ (lower panels) with associated medians (gray lines). Note that the scale of the x axis is not constant across plots.

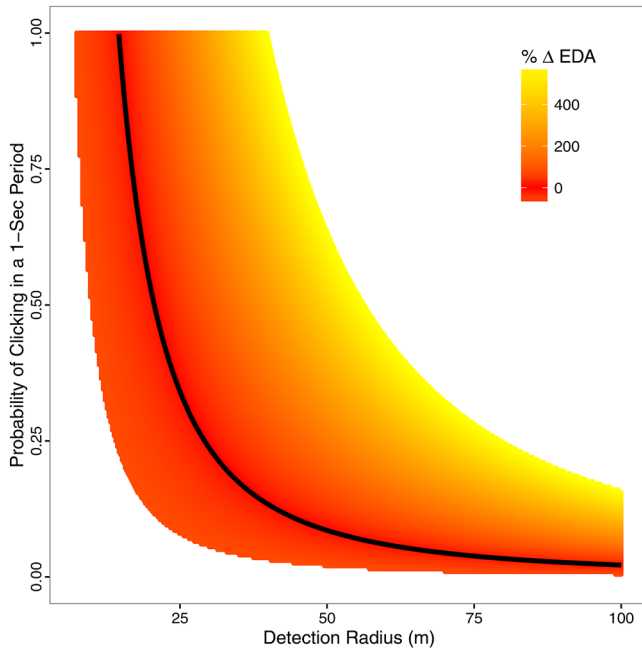


FIG. 7. (Color online) Parameter space of the detection radius (v) and the probability of clicking within a 1-s period (p) consistent with the model estimate of the EDA ($\hat{v}p$). The black line indicates the median estimate and all possible combinations of v and p that fall within the 95% credibility interval of the model estimate of the EDA are shown. The color scale indicates the percent change in EDA relative to the estimate, with darker colors indicating values closest to the median.

to other species and regions where researchers wish to transition from aerial surveys to passive acoustic methods for monitoring trends in cetacean abundance.

We used objective interpolation to estimate the spatial density of the harbor porpoise across our study area from

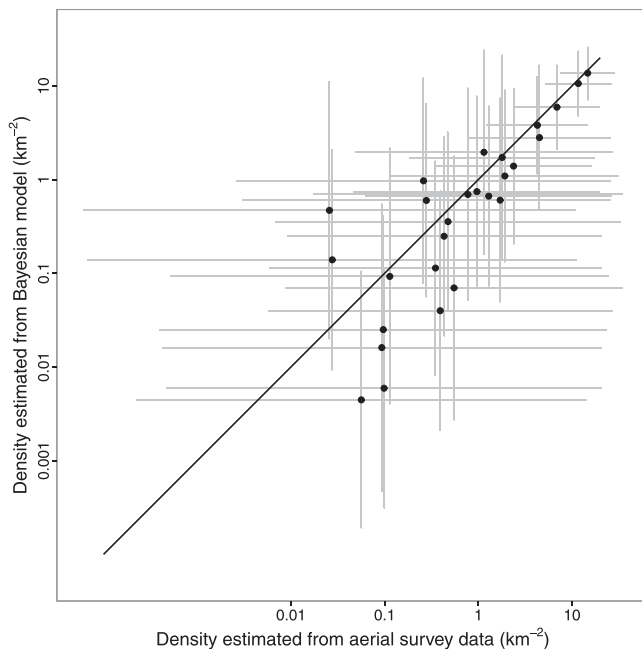


FIG. 8. Mean harbor porpoise density (km^{-2}) at the location of each C-POD on each day ($N=27$) as estimated by the objective interpolation of aerial survey data (x axis) and as estimated by the Bayesian model (y axis) with associated 95% confidence and credibility intervals for the two approaches. The one-to-one line (black line) indicates perfect agreement.

line-transect aerial surveys. Aerial survey data are inherently highly variable, due to both process (e.g., patchy harbor porpoise distribution) and observation (intermittent visual availability, observer perception) errors. Multiple aerial surveys conducted on a single day would likely reduce the uncertainty associated with point estimates of harbor porpoise density at individual C-POD locations; however, this would be an expensive and logistically difficult undertaking. Due to the variability in aerial survey data, it is difficult to interpolate these data with a high degree of certainty. Our adaptation of objective interpolation for this task used the underlying statistics of the data to determine the length scales of interpolation, allowing us to interpolate across the study area while recognizing the uncertainty associated with doing so. This approach also avoided oversmoothing the aerial survey data and preserved the patchy harbor porpoise distributions observed during aerial surveys.

Daily and monthly estimates of abundance generated using visual and passive acoustic data had similar means; however, uncertainty was much greater in the passive acoustic estimates than in the visual estimates of abundance (Fig. 9, first and second panels). Uncertainty in the passive acoustic abundance estimate is large because of variability in both the passive acoustic records and in the aerial survey data; since the passive acoustic abundance estimate relies on the EDA estimated using aerial survey data it effectively incorporates all uncertainty in both survey methods. However, the mean abundance estimates were relatively stable over time, giving us confidence that this method works albeit with large uncertainties.

Ideally, the EDA should be estimated separately for each instrument and each set of environmental conditions (Kyhn *et al.*, 2012). Harbor porpoise click propagation can change with factors including temperature, depth, salinity, and substrate type (DeRuiter *et al.*, 2010) resulting in different EDAs. Similarly, harbor porpoise foraging and echolocation behavior can vary with time of day, season, and location (Carlstrom, 2005). With our limited dataset, we were not able to estimate EDAs specific to each C-POD. If enough paired surveys (e.g., $N=10$) were conducted, a hierarchical framework could be used to estimate an EDA specific to each C-POD. It is possible that some of the variance in the posterior density distributions is due to this unaccounted for source of variation in detectability, since, for example, sensors in shallow water may have different EDAs from sensors in deep water.

If we assumed that detectability were constant over time (i.e., no seasonal changes in echolocation click rates or detectability), our estimated EDA could be used to estimate harbor porpoise abundance in our study area at times when visual surveys were not conducted (Fig. 9, second and third panels). If we wished to estimate trends in abundance rather than absolute abundance, we could ignore the uncertainty in the estimated EDA, though changes in the EDA over time and space would still be an issue. When the uncertainty in the EDA was not included (Fig. 9, fourth panel) the uncertainty in the passive acoustic abundance estimates was considerably lower and more in line with that of the visual abundance estimates. In our study, aerial surveys were

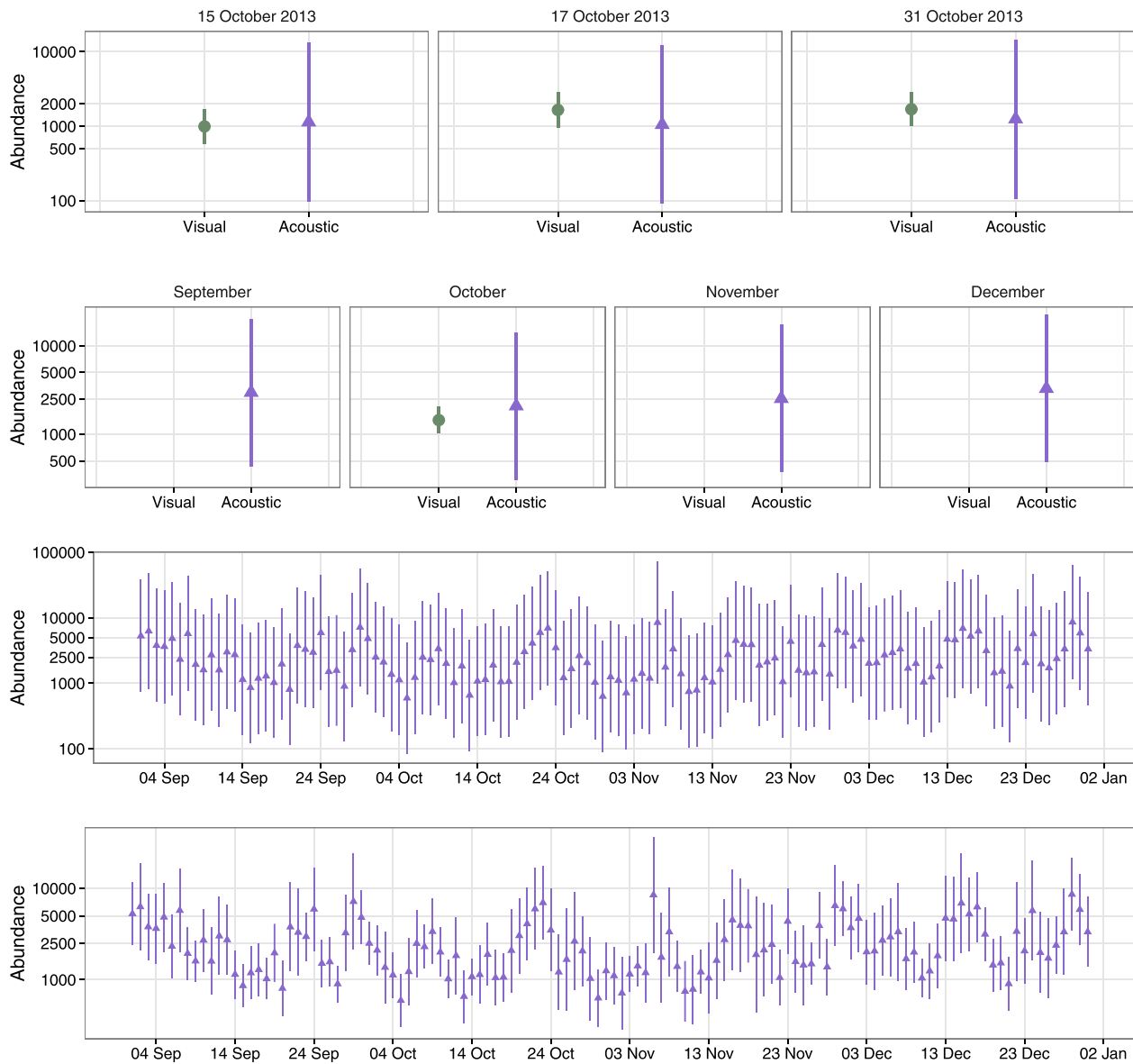


FIG. 9. (Color online) Visual (green circles) and passive acoustic (purple triangles) estimates of harbor porpoise abundance in the Monterey Bay study area with 95% confidence intervals calculated for each of the three days of effort used in this study (first panel), each month for which passive acoustic data were available (second panel), and for each day on which passive acoustic data were available with error in the estimates of $\hat{\nu}\rho$ and $\hat{g}(0)$ included (third panel) and without error in the estimates of $\hat{\nu}\rho$ and $\hat{g}(0)$ included (fourth panel).

conducted on days with relatively low recorded echolocation activity (Fig. 9, fourth panel), indicating that the visual estimate may be an underestimate of the average abundance of harbor porpoise in this area.

V. CONCLUSIONS

Paired visual and passive acoustic surveys can be used to estimate the detectability of cetaceans. Our study demonstrates that using this technique, it is possible to generate passive acoustic estimates of harbor porpoise abundance that are consistent with aerial survey estimates of abundance. This approach is most feasible in areas with high cetacean densities and may not work in regions where very few animals are observed during visual surveys and reliable interpolation of visual survey data are not possible. For paired survey parameter estimation to be used effectively, more

visual surveys are needed to increase the sample size of the paired dataset and decrease the uncertainty in the estimated EDA. With enough simultaneous aerial surveys, it might be possible to estimate EDAs specific to individual passive acoustic sensors. This would allow parameters to be estimated for instruments in different water depths and with different substrate types, facilitating the extrapolation of estimated parameters to regions where paired surveys have not been conducted.

ACKNOWLEDGMENTS

We thank the Moss Landing Marine Laboratories Small Boat Center, especially Captain John Douglas, for their generous assistance with field operations. Scientific divers Scott Gabara, Jasmine Ruvalcaba, and Diana Steller facilitated the deployment and retrieval of C-POD moorings.

We thank Aspen Helicopters, Inc. and pilot Barry Hansen and visual observers Melinda Nakagawa, Scott Benson, Katherine Whitaker, Kelly Newton, and Deasy Lontoh for participating in visual surveys. Jennifer Secoy Krach provided crucial logistical support to E.K.J. during fieldwork in Monterey Bay. Tim Gerrodette and Peter Franks provided helpful advice regarding the hypotheses and approaches used in this study, Sean Crosby facilitated the application of objective interpolation, Jeff Laake assisted with visual line-transect analyses, and Brice Semmens and Jeff Moore guided the implementation of the Bayesian modeling. We thank three anonymous reviewers for their thoughtful comments and suggestions on a previous version of this manuscript. C-POD deployments were conducted under Monterey Bay National Marine Sanctuary Permit No. MBNMS-2011-026. Aerial surveys were conducted under National Marine Sanctuary Permit Nos. MULTI-2008-03 and MULTI-2013-09 and National Marine Fisheries Service Permit No. 14097. We thank the California Energy Commission for funding the research presented in this report and the California Institute for Energy and Environment for coordinating the management of this project. E.K.J. was also supported by the NSF Integrative Graduate Education and Research Traineeship and the NSF Graduate Research Fellowship Program.

- Akamatsu, T., Teilmann, J., Miller, L. A., Tougaard, J., Dietz, R., Wang, D., Wang, K. X., Siebert, U., and Naito, Y. (2007). "Comparison of echolocation behaviour between coastal and riverine porpoises," *Deep Sea Res. Part II* **54**, 290–297.
- Anderson, D. (2014). "Harbor porpoise return to the South Puget Sound: Using bioacoustic methods to monitor a recovering population," MS thesis, Evergreen State College, Olympia, WA.
- Au, W., Kastelein, R., Rippe, T., and Schooneman, N. (1999). "Transmission beam pattern and echolocation signals of a harbor porpoise (*Phocoena phocoena*)," *J. Acoust. Soc. Am.* **106**, 3699–3705.
- Bailey, H., Clay, G., Coates, E. A., Lusseau, D., Senior, B., and Thompson, P. M. (2010). "Using T-PODs to assess variations in the occurrence of coastal bottlenose dolphins and harbour porpoises," *Aquatic Conserv: Mar. Freshw. Ecosyst.* **20**, 150–158.
- Barlow, J. (1988). "Harbor porpoise, *Phocoena phocoena*, abundance estimation for California, Oregon, and Washington: I. Ship surveys," *Fish. Bull.* **86**, 417–432.
- Barlow, J., and Forney, K. A. (1994). "An assessment of the 1994 status of harbor porpoise in California," U.S. Dept. of Commerce NOAA Tech. Memo., NOAA-TM-NMFS-SWFSC-205.
- Barlow, J., and Hanan, J. (1995). "An assessment of the status of harbor porpoise in central California," Rept. Int. Whal. Special Issue **16**, 123–140.
- Becker, E., Foley, D., Forney, K., Barlow, J., Redfern, J., and Gentemann, C. (2012). "Forecasting cetacean abundance patterns to enhance management decisions," *Endanger. Species Res.* **16**, 97–112.
- Becker, E., Forney, K., Ferguson, M., Foley, D., Smith, R., Barlow, J., and Redfern, J. (2010). "Comparing California current cetacean–habitat models developed using *in situ* and remotely sensed sea surface temperature data," *Mar. Ecol. Prog. Ser.* **413**, 163–183.
- Brandt, M., Diederichs, A., Betke, K., and Nehls, G. (2011). "Responses of harbour porpoises to pile driving at the Horns Rev II offshore wind farm in the Danish North Sea," *Mar. Ecol. Prog. Ser.* **421**, 205–216.
- Brandt, M. J., Hansen, S., Diederichs, A., and Nehls, G. (2014). "Do man-made structures and water depth affect the diel rhythms in click recordings of harbor porpoises (*Phocoena phocoena*)?," *Mar. Mamm. Sci.* **30**, 1109–1121.
- Bretherton, F. P., Davis, R. E., and Fandry, C. B. (1976). "A technique for objective analysis and design of oceanographic experiments applied to MODE-73," *Deep-Sea Res.* **23**, 559–582.
- Buckland, S. T., Anderson, D. R., Burnham, K. P., Laake, J. L., Borchers, D. L., and Thomas, L. (2001). *Introduction to Distance Sampling* (Oxford University Press, Oxford), 446 pp.
- Calambokidis, J., and Barlow, J. (1991). "Chlorinated hydrocarbon concentrations and their use for describing population discreteness in harbor porpoises from Washington, Oregon, and California," in *Proceedings of the Second Marine Mammal Stranding Workshop*, Marine Mammal Strandings in the United States, Miami, Florida (December 3–5, 1987), U.S. Department of Commerce NOAA Tech. Memo., NMFS-98.
- Calambokidis, J., Peard, J., Steiger, G. H., Cubbage, J. C., and DeLong, R. L. (1984). "Chemical contaminants in marine mammals from Washington state," U.S. Department of Commerce NOAA Tech. Memo., NOS-OMS-6.
- Calambokidis, J., Speich, S. M., Peard, J., Steiger, G. H., Cubbage, J. C., Fry, D. M., and Lowenstine, L. J. (1985). "Biology of Puget Sound marine mammals and marine birds: Population health and evidence of pollution effects," U.S. Department of Commerce NOAA Tech. Memo., NOS-OMA-18.
- Carlstrom, J. (2005). "Diel variation in echolocation behavior of wild harbor porpoises," *Mar. Mamm. Sci.* **21**, 1–12.
- Carretta, J., Oleson, E. M., Weller, D. W., Lang, A. R., Forney, K., Baker, J., Muto, M. M., Hanson, B., Orr, A. J., Huber, H., Lowry, M. S., Barlow, J., Moore, J. E., Lynch, D., Carswell, L., and Brownell, R. L. (2015). "U.S. Pacific Marine Mammal Stock Assessments: 2014," U.S. Department of Commerce, NOAA Tech. Memo., NOAA-TM-NMFS-SWFSC-549.
- Carretta, J. V., Taylor, B. L., and Chivers, S. J. (2001). "Abundance and depth distribution of harbor porpoise (*Phocoena phocoena*) in northern California determined from a 1995 ship survey," *Fish. Bull.* **99**, 1–11.
- Carstensen, J., Henriksen, O., and Teilmann, J. (2006). "Impacts of offshore wind farm construction on harbour porpoises: Acoustic monitoring of echolocation activity using porpoise detectors (T-PODs)," *Mar. Ecol. Prog. Ser.* **321**, 295–308.
- Chivers, S. J., Dizon, A. E., Gearin, P. J., and Robertson, K. M. (2002). "Small-scale population structure of eastern North Pacific harbour porpoises (*Phocoena phocoena*) indicated by molecular genetic analyses," *J. Cetacean Res. Manage.* **4**, 111–122.
- Clausen, K. T., Wahlberg, M., Beedholm, K., Deruiter, S., and Madsen, P. T. (2010). "Click communication in harbour porpoises *Phocoena phocoena*," *Bioacoustics* **20**, 1–28.
- Cotter, M. P., Maldini, D., and Jefferson, T. A. (2011). "'Porpicide' in California: Killing of harbor porpoises (*Phocoena phocoena*) by coastal bottlenose dolphins (*Tursiops truncatus*)," *Mar. Mam. Sci.* **28**, E1–E15.
- Dähne, M., Gilles, A., Lucke, K., Peschko, V., Adler, S., Krügel, K., Sundermeyer, J., and Siebert, U. (2013a). "Effects of pile-driving on harbor porpoises (*Phocoena phocoena*) at the first offshore wind farm in Germany," *Environ. Res. Lett.* **8**, 025002.
- Dähne, M., Verfuß, U. K., Brandecker, A., Siebert, U., and Benke, H. (2013b). "Methodology and results of calibration of tonal click detectors for small odontocetes (C-PODs)," *J. Acoust. Soc. Am.* **134**, 2514–2522.
- DeRuiter, S. L., Hansen, M., Koopman, H. N., Westgate, A. J., Tyack, P. L., and Madsen, P. T. (2010). "Propagation of narrow-band-high-frequency clicks: Measured and modeled transmission loss of porpoise-like clicks in porpoise habitats," *J. Acoust. Soc. Am.* **127**, 560–567.
- Forney, K. A. (2000). "Environmental models of cetacean abundance: Reducing uncertainty in population trends," *Cons. Bio.* **14**, 1271–1286.
- Forney, K., Carretta, J. V., and Benson, S. R. (2014). "Preliminary estimates of harbor porpoise abundance in Pacific Coast waters of California, Oregon and Washington, 2007–2012," U.S. Department of Commerce NOAA Tech. Memo. NMFS-SWFSC-537.
- Forney, K., Ferguson, M. C., Becker, E. A., Fiedler, P. C., Redfern, J. V., Barlow, J., Vilchis, I. L., and Ballance, L. T. (2012). "Habitat-based spatial models of cetacean density in the eastern Pacific Ocean," *Endanger. Species Res.* **16**, 113–133.
- Forney, K., Hanan, D. A., and Barlow, J. (1991). "Detecting trends in harbor porpoise abundance from aerial surveys using analysis of covariance," *Fish. Bull.* **89**, 1–11.
- Forney, K. A., Benson, S. R., and Cameron, G. A. (2001). "Central California gillnet effort and bycatch of sensitive species," in *Proceedings of the Seabird Bycatch: Trends, Roadblocks, and Solutions*, University of Alaska Sea Grant, AK-SG-01-01.
- Gallus, A., Dähne, M., Verfuß, U. K., Bräger, S., Adler, S., Siebert, U., and Benke, H. (2012). "Use of static passive acoustic monitoring to assess the status of the 'Critically Endangered' Baltic harbour porpoise in German waters," *Endanger. Species Res.* **18**, 265–278.

- Gandin, L. S. (1965). *Objective Analysis of Meteorological Fields* (Israel Program for Scientific Translations, Jerusalem), 242 pp.
- Jacobson, E. K., Forney, K. A., and Harvey, J. T. (2014). "Acoustic evidence that harbor porpoises (*Phocoena phocoena*) avoid bottlenose dolphins (*Tursiops truncatus*)," *Mar. Mam. Sci.* **31**, 386–397.
- Jaramillo-Legorreta, A., Cardenas-Hinojosa, G., Nieto-Garcia, E., Rojas-Bracho, L., Ver Hoef, J., Moore, J., Tregenza, N., Barlow, J., Gerrodette, T., Thomas, L., and Taylor, B. (2016). "Passive acoustic monitoring of the decline of Mexico's critically endangered vaquita," *Cons. Bio.* doi:10.1111/cobi.12789.
- Jefferson, T., Curry, B., and Black, N. (1994). "Harbor porpoise mortality in the Monterey Bay halibut gillnet fishery, 1989," *Rep. Int. Whaling Comm.* **15**, 445–448.
- Keener, W., Szczepaniak, I., Adam, Ü., and Webber, M. (2011). "First records of anomalously white harbour porpoises (*Phocoena phocoena*) from the Pacific Ocean," *J. Mar. Ani. Ecol.* **4**, 19–24.
- Koblitz, J. C. (2015). "Determinants for the detection function of passive acoustic data loggers," in *The 5th International Workshop on Detection, Classification, Localization, and Density Estimation of Marine Mammals using Passive Acoustics*, San Diego, CA.
- Koblitz, J. C., Wahlberg, M., and Stiltz, P. (2012). "Asymmetry and dynamics of a narrow sonar beam in an echolocating harbor porpoise," *J. Acoust. Soc. Am.* **131**, 2315–2324.
- Kyhn, L. A., Tougaard, J., Thomas, L., Duve, L. R., Stenback, J., Amundin, M., Desportes, G., and Teilmann, J. (2012). "From echolocation clicks to animal density—Acoustic sampling of harbor porpoises with static data-loggers," *J. Acoust. Soc. Am.* **131**, 550–560.
- Laake, J. L., Calambokidis, J., Osmek, S. D., and Rugh, D. J. (1997). "Probability of detecting harbor porpoise from aerial surveys: Estimating $g(0)$," *J. Wildl. Manage.* **61**, 63–75.
- Linnenschmidt, M., Teilmann, J., Akamatsu, T., Dietz, R., and Miller, L. A. (2012). "Biosonar, dive, and foraging activity of satellite tracked harbor porpoises (*Phocoena phocoena*)," *Mar. Mamm. Sci.* **29**, E77–E97.
- Marques, T. A., Thomas, L., Martin, S. W., Mellinger, D. K., Ward, J. A., Moretti, D. J., Harris, D., and Tyack, P. L. (2013). "Estimating animal population density using passive acoustics," *Biol. Rev.* **88**, 287–309.
- Marques, T. A., Thomas, L., Ward, J., DiMarzio, N., and Tyack, P. L. (2009). "Estimating cetacean population density using fixed passive acoustic sensors: An example with Blainville's beaked whales," *J. Acoust. Soc. Am.* **125**, 1982–1994.
- McIntosh, P. C. (1990). "Oceanographic data interpolation: Objective analysis and splines," *J. Geophys. Res.: Oceans* (1978–2012), **95**, 13529–13541.
- Mellinger, D. K., Stafford, K. M., Moore, S., Dziak, R. P., and Matsumoto, H. (2007). "Fixed passive acoustic observation methods for cetaceans," *J. Oceanogr.* **20**, 36–45.
- Miller, D. L. (2015). "Distance: Distance sampling detection function and abundance estimation," R package version 0.9.4. <https://CRAN.R-project.org/package=Distance> (Last viewed 2 January 2017).
- R Core Team (2016). "R: A language and environment for statistical computing," R Foundation for Statistical Computing, Vienna, Austria. URL <https://www.R-project.org/> (Last viewed 2 January 2017).
- Raum-Suryan, K. L., and Harvey, J. T. (1998). "Distribution and abundance of and habitat use by harbor porpoise, *Phocoena phocoena*, off the northern San Juan Islands, Washington," *Fish. Bull.* **96**, 808–822.
- Seber, G. A. F. (1982). *The Estimation of Animal Abundance*, 2nd ed. (Griffin, London), 654 pp.
- Su, Y., and Yajima, M. (2015). "R2jags: Using R to Run 'JAGS,'" R package version 0.5-7. <https://CRAN.R-project.org/package=R2jags> (Last viewed 2 January 2017).
- Thompson, P. M., Brookes, K. L., Graham, I. M., Barton, T. M., Needham, K., Bradbury, G., and Merchant, N. D. (2013). "Short-term disturbance by a commercial two-dimensional seismic survey does not lead to long-term displacement of harbour porpoises," *Proc. R. Soc. B* **280**, 1–8.
- Thomson, R. E., and Emery, W. J. (2014). *Data Analysis Methods in Physical Oceanography* (Elsevier, New York).
- Tregenza, N. (2012). *CPOD.exe: A Guide for Users*. <http://www.chelonia.co.uk/downloads/CPOD.pdf> (Last viewed 2 January 2017).
- Verfuß, U. K., Honnef, C., Meding, A., Dähne, M., Mundry, R., and Benke, H. (2007). "Geographical and seasonal variation of harbor porpoise (*Phocoena phocoena*) presence in the German Baltic Sea revealed by passive acoustic monitoring," *J. Mar. Biol. Ass. U.K.* **87**, 165–176.
- Wilkin, S. M., Cordaro, J., and Gulland, F. (2012). "An unusual mortality event of harbor porpoises (*Phocoena phocoena*) off Central California: Increase in blunt trauma rather than an epizootic," *Aquat. Mamm.* **38**, 301–310.
- Williamson, L. D., Brookes, K. L., Scott, B. E., Graham, I. M., Bradbury, G., Hammond, P. S., and Thompson, P. M. (2016). "Echolocation detections and digital video surveys provide reliable estimates of the relative density of harbour porpoises," *Methods Ecol. Evol.* **7**, 762–769.
- Wisniewska, D. M., Johnson, M., Teilmann, J., Rojano-Doñate, L., Shearer, J., Sveegaard, S., Miller, L. A., Siebert, U., and Madsen, P. T. (2016). "Ultra-high foraging rates of harbor porpoises make them vulnerable to anthropogenic disturbance," *Curr. Biol.* **26**, 1441–1446.